JACS
JOURNAL OF THE AMERICAN CHEMICAL SOCIETY

Communication

pubs.acs.org/JACS

Self-Healing Multiphase Polymers via Dynamic Metal–Ligand Interactions

Davoud Mozhdehi, Sergio Ayala, Olivia R. Cromwell, and Zhibin Guan*

Department of Chemistry, University of California, Irvine, California 92697, United States

Supporting Information

ABSTRACT: A new self-healing multiphase polymer is developed in which a pervasive network of dynamic metal–ligand (zinc–imidazole) interactions are programmed in the soft matrix of a hard/soft two-phase brush copolymer system. The mechanical and dynamic properties of the materials can be tuned by varying a number of molecular parameters (e.g., backbone/brush degree of polymerization and brush density) as well as the ligand/metal ratio. Following mechanical damage, these thermoplastic elastomers show excellent self-healing ability under ambient conditions without any intervention.

Self-healing materials are under intense development recently because self-healing ability would improve the safety, lifetime, energy efficiency, and environmental impact of manmade materials. Several self-healing strategies have been reported for polymer systems, such as the incorporation of healing agents[1,2] and the use of reversible and irreversible covalent bonds[2−5] as well as dynamic noncovalent bonding interactions as the healing motifs.[6−10] Metal–ligand (M–L) complexes are promising candidates as dynamic healing motifs because the thermodynamic and kinetic parameters of M–L complexes are tunable over a broad range, which could potentially yield materials with highly tunable mechanical properties.[11,12] Furthermore, M–L interactions are less sensitive to moisture than hydrogen bonds, which should be advantageous for practical applications. Several self-healing gels and solid materials have been reported by using reversible metal–ligand interactions.[13−18] For self-healing solid materials, the most commonly utilized M–L systems involve multidentate nitrogen-based aromatic ligands, such as terpyridines.[15,16] These systems have relatively high M–L association constants and tend to phase separate with the M–L complexes residing in hard glassy or crystalline domains. Because of the high association constants and the fact that the M–L complexes either form ionic clusters or reside in the hard, nondynamic domains, external energy such as heat[16] or light[15] must be required to reversibly dissociate the M–L complexes to induce self-healing.

To realize a spontaneous self-healing M–L polymer, we decided to choose a highly dynamic M–L interaction, Zn^{2+}–imidazole, as the healing motif. Compared to the previously utilized multidentate ligands, imidazole has a relatively small binding constant to metal ions, and its M–L complexes have fast exchange kinetics.[19] In particular, Zn^{2+}–imidazole interactions are ubiquitous in biological systems, where the ligand exchange is known to have fast dynamics.[20] In addition, to combine good mechanical properties with spontaneous self-healing capability under ambient conditions, we designed a microphase-separated soft/hard two-phase polymer system with the M–L complexes strategically embedded in the soft matrix having low glass transition temperature (T_g) (Figure 1).

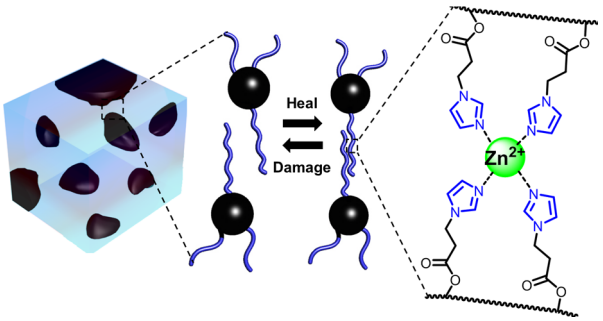

Figure 1. Design concept for the multiphasic spontaneous self-healing materials using metal–ligand interaction as the dynamic motif.

Following our previous design of a spontaneous self-healing hydrogen-bonding polymer,[21] we chose a brush polymer architecture to demonstrate our two-phase, M–L system for self-healing under ambient conditions. Specifically, a glassy polystyrene (PS) was used as the backbone, from which multiple imidazole-containing brushes were grown. The addition of Zn^{2+} salts to the brush polymer solution induced complexation with the imidazole moieties. Upon drying, the system microphase separated into two phases with the hard PS domain contributing to the stiffness and modulus of the resulting material. Importantly, the dynamic Zn^{2+}–imidazole complexes reside in the soft matrix (Figure 1). With a combination of fast ligand exchange kinetics for Zn^{2+}–imidazole complex and the dynamics of the soft polymer matrix, we envision that this system can self-heal in the solid state with minimal intervention.

The synthesis of the imidazole-containing brush polymers, **ICPs**, is described in Scheme 1. The imidazole-containing acrylate monomer, **IMZa** (**2**), was synthesized via Michael addition of imidazole to 1,4-butanediol diacrylate (Scheme 1a). The spacer between the imidazole ring and the acrylate moiety is necessary for lowering the glass transition temperature and enhancing the dynamics of the ligands in the soft polymer

Received: September 19, 2014
Published: October 28, 2014

   dx.doi.org/10.1021/ja5097094 | J. Am. Chem. Soc. 2014, 136, 16128–16131

Scheme 1. Synthesis of the Imidazole-Containing Monomer and Brush Copolymers[a]

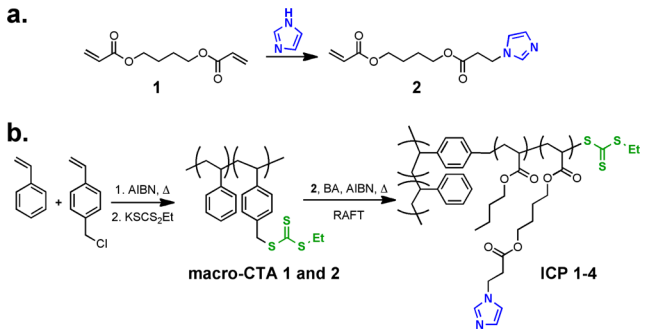

[a](a) Synthesis of imidazole acrylate monomer, **IMZa** (**2**). (b) Synthesis of **ICP**s. Styrene was first copolymerized with 4-vinylbenzyl chloride via free-radical polymerization, followed by post-functionalization of benzyl chloride to form macro-CTAs. **ICP**s were synthesized by growing copolymer brushes of BA and **IMZa** using RAFT controlled radical polymerization technique.

matrix (T_g of copolymer ≈ −38 °C) before the addition of metal (Supporting Information, Figure S11).

Reversible addition−fragmentation chain transfer polymerization (RAFT) was chosen to synthesize our brush copolymers.[22] The PS macro-chain transfer agent (macro-CTA) was synthesized by free radical copolymerization of styrene and varied amount of 4-vinylbenzyl chloride to obtain PS backbone with controlled amount of benzyl chloride incorporation (Scheme 1b). This polymer was further functionalized by treating with in situ generated potassium ethyl trithiocarbonate salt to introduce RAFT chain transfer sites.[23] Two PS macro-CTAs were synthesized with the PS backbone of ∼140 repeating units and the density of the RAFT chain transfer group of 5% and 10%, respectively. These macro-CTAs were subsequently used to initiate RAFT copolymerization of *n*-butyl acrylate (BA) and the custom-made monomer, **IMZa** (**2**), to grow multiple brushes from the PS backbone. The brush degree of polymerization was controlled at ∼180 repeating units and the imidazole mole percent at 25% and 35%, respectively. To avoid the complication of hydrogen bonding in self-healing studies, we decided to use the N-substituted imidazole and BA to form our **ICP**s. For comparison, two control polymers were also synthesized: **Control-1** is a brush polymer without any imidazole (i.e., only BA homopolymer on the brushes). **Control-2** does not have the brush architecture; instead, it is a linear copolymer of BA and **IMZa**. The composition of all **ICP**s and control samples are summarized in Table 1. The synthesis and full characterizations of both the monomer **2** and all polymers are detailed in the Supporting Information.

For M−L complexation, zinc di[bis(trifluoromethylsulfonyl)-imide], $Zn(NTf_2)_2$, was chosen as the Zn^{2+} source for its good solubility and thermal stability, as well as the high mobility of the counterion, NTf_2^-, in the solid state. With the delocalized charge, bulky size, and unique shape, NTf_2^- counterion disfavors clustering of charged species in the solid state.[24,25] Without the addition of metal ions, the **ICP**s are viscous oils with no appreciable mechanical properties. Upon addition of $Zn(NTf_2)_2$ and removal of solvent, they form robust non-tacky elastomers with tunable mechanical properties. Thermogravimetric analysis (TGA) confirmed the complete removal of solvent (Supporting Information, Figure S12).

Table 1. Molecular Compositions of ICP 1−4 and Control Samples

sample	backbone repeat units[a]	CTA sites[b]	brush repeat units[b]	mol % of IMZa[b,c]
ICP-1	140	14	180	25
ICP-2	140	14	167	33
ICP-3	139	7	167	25
ICP-4	139	7	160	34
Control-1	140	14	190	0
Control-2			170	35

[a]Calculated from size exclusion chromatography (SEC) using polystyrene standards in THF. [b]Estimated from ^{1}H NMR. [c]mol %, calculated from $N_{IMZa}/(N_{IMZa} + N_{BA}) \times 100$, where N is the number of repeat units for each monomer.

The phase morphology of **ICP**s−$Zn(NTf_2)_2$ samples in solid state was investigated by small-angle X-ray scattering (SAXS) and transmission electron microscopy (TEM). As shown in Figure 2a for **ICP-4** (L/Zn = 4.0), an intense broad peak in the

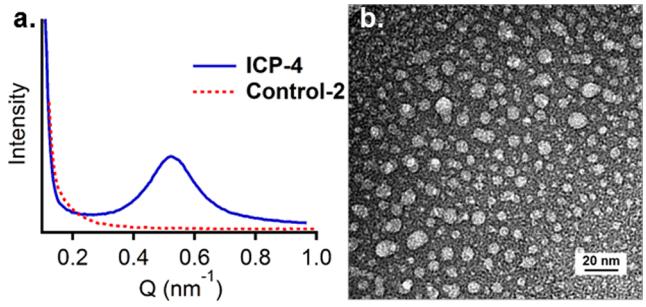

Figure 2. Morphological characterization of **ICP**s−$Zn(NTf_2)_2$ samples. (a) Small angle X-ray scattering (SAXS) supports the microphase separated morphology with inter-domain spacing between 7 and 20 nm for **ICP-4** (L/M = 4.0). The control sample (**Control-2**) does not show any scattering peak. (b) TEM imaging confirms a microphase-separated structure with a spherical PS core dispersed in a soft BA/**IMZa** matrix, which was selectively stained with uranyl acetate.

SAXS spectrum indicates the presence of well-defined spherical form-factor domains with inter-domain spacing ranging between 7 and 20 nm. In contrast, **Control-2**, which does not contain PS backbone, did not show any scattering peak, suggesting that the $Zn(NTf_2)_2$−imidazole complex does not form large ionic clusters or microphase separation in the solid state.[25] TEM provides further evidence for a two-phase morphology of **ICP**s (Figure 2b). Consistent with the SAXS data, spherical PS nanodomains with size ∼10 nm are dispersed in a continuous matrix of soft brushes containing dynamic zinc−imidazole complexes.

The designed M−L multiphase polymers show characteristic thermoplastic elastomer (TPE) behavior with tunable mechanical properties by controlling several molecular parameters (Figure 3a). Consistent with our multiphase design strategy, the PS hard phase contributes to the high Young's modulus and TPE-like behavior. For comparison, the **Control-2** samples, which do not contain PS backbones, have lower Young's modulus and do not show the TPE behavior (Supporting Information, Figure S13). The mechanical performance can be tuned by adjusting three molecular parameters: the percent incorporation of **IMZa**, the ratio of imidazole to zinc (L/Zn), and the volume fraction of hard phase or brush density. For

dx.doi.org/10.1021/ja5097094 | J. Am. Chem. Soc. 2014, 136, 16128−16131

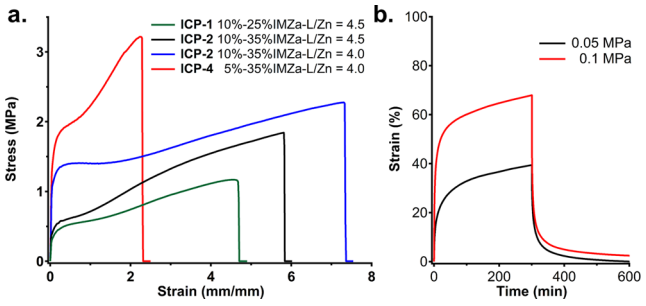

Figure 3. (a) Static tensile tests of **ICPs**–$Zn(NTf_2)_2$ samples. It shows the TPE-like stress–strain behavior, and the mechanical properties can be tuned over a wide range by changing three molecular parameters, the **IMZa** incorporation percentage, the ratio of imidazole to zinc (L/Zn), and the brush density. (b) Creep-recovery experiments showing **ICP-4**–$Zn(NTf_2)_2$, with L/Zn = 4.0 after application of constant stress for 300 min followed by relaxation of stress.

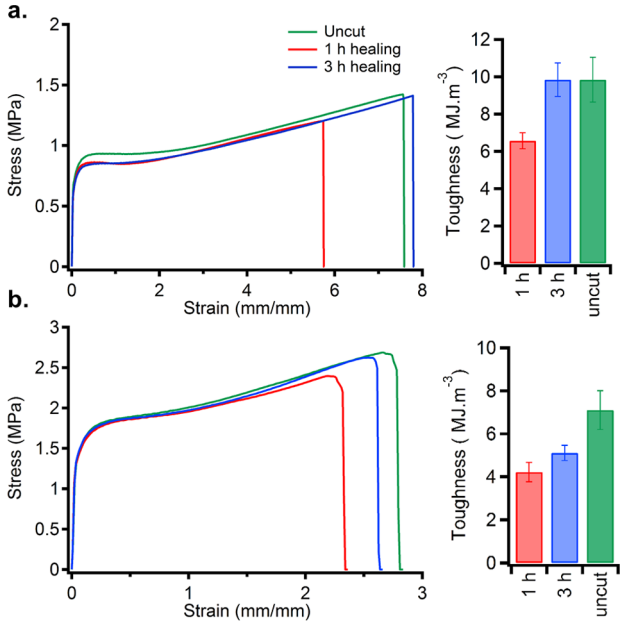

Figure 4. Self-healing tests for **ICPs**–$Zn(NTf_2)_2$ samples at room temperature with ambient humidity. (a) Stress–strain curve for **ICP-2** L/Zn = 4.0. (b) Stress–strain curve for **ICP-4** L/Zn = 4.0. The bar graph summarizes the toughness recovery for each sample. Error bars are standard deviation for three measurements.

example, increasing the **IMZa** incorporation from 25% (Figure 3a, green curve) to 35% (Figure 3a, black curve) increases the yield strength, tensile strength, and extensibility. Decreasing the L/Zn from 4.5 (Figure 3a, black curve) to 4.0 (Figure 3a, blue curve) by adding more Zn^{2+} also significantly improves mechanical properties of **ICPs** by increasing the cross-linking density of polymer samples.[26] Finally, consistent with our previous report,[21] increasing the volume fraction of the PS hard phase by reducing the brush density from 10% (Figure 3a, blue curve) to 5% (Figure 3a, red curve) resulted in an increase in Young's modulus, yield strength, and tensile strength while decreasing the extensibility of material. A complete summary of the mechanical properties of **ICPs**–$Zn(NTf_2)_2$ and **Control-2** polymers with L/Zn ratio of 4.0 and 4.5 is included in the Supporting Information (Table S3). Without any imidazole moiety, **Control-1** only formed viscous oil and its mechanical properties remained almost unchanged with the addition of $Zn(NTf_2)_2$, as shown by oscillatory rheology (Supporting Information, Figure S14).

The M–L multiphase polymers also exhibit reasonable creep-resistance despite the fact that the soft polymer matrix is only held together by transient dynamic M–L cross-links (Figure 3b). At 24 °C, a stress of 5×10^4 Pa applied to **ICP-4** with L/Zn ratio of 4.0 for 300 min resulted in the final strain of 39%, which increased at a characteristic rate of 1.8% per hour. After releasing the applied stress, the sample completely recovered its dimension with negligible residual strain (<1%). Application of a higher stress (1.0×10^5 Pa) for the same time duration led to a strain of 70% with an incremental increase of 2.2% per hour. Release of stress left a residual strain of less than 5%. As expected, an elastomeric network that is held together purely by transient dynamic bonds will not be able to maintain static high load indefinitely.

With the dynamic Zn^{2+}-imidazole complexes residing in the dynamic soft phase of a two-phase polymer system, our M–L system showed excellent self-healing property in the solid state. The **ICP-2** and **ICP-4** with L/Zn of 4.0 were chosen as representative samples for the self-healing test because of their better mechanical properties (Figure 4). Samples used in self-healing studies were annealed by slowly cooling the samples from 100 °C to room temperature over 12 h to minimize any residual stress during compression molding. Following a literature protocol,[15] we then made a well-defined cut to the depth of 70–90% of the sample thickness. The two cut interfaces were brought back together for 1 min and allowed to heal under ambient conditions (room temperature in air) without any treatment.

The damaged samples showed excellent healing with time. For all healing times, stress–strain curves show characteristic TPE behavior and follow closely the shapes of the original uncut samples. Remarkably, the damaged samples not only recovered the Young's modulus and yield stress quickly, but also recovered toughness almost quantitatively in 3 h. In contrast, previous M–L systems utilizing terpyridine–metal interactions required light-converted local heat,[15] relatively long healing time under heat,[16] or solvent exposure to induce healing.[17] The observed efficient healing proves our hypothesis that incorporation of pervasive dynamic M–L interactions in the soft-phase of a multiphase polymer can result in mechanically robust materials with efficient self-healing under ambient conditions. The healing efficiencies of metal–ligand system even surpasses our previous reported hydrogen bonding system.[21] Notably, our M–L polymers heal efficiently at ambient conditions without showing sensitivity to moisture, which is advantageous to hydrogen-bonding based self-healing polymers that are usually more sensitive to moisture.

In summary, we have demonstrated a new self-healing multiphase polymer by strategically programming a pervasive network of dynamic metal–ligand (zinc–imidazole) interactions in the soft matrix of a hard/soft two-phase brush copolymer system. The mechanical and dynamic properties of the materials can be conveniently tuned by varying several molecular parameters (such as the backbone composition and degree of polymerization, the brush density, and the ligand density) as well as the L/M ratio. Our multiphase M–L polymers show excellent self-healing properties under ambient conditions with minimal intervention. Compared to hydrogen-bonding based self-healing systems, the M–L system may offer advantages of being less moisture sensitive and having a broad range of tunability of thermodynamics and kinetics. Several

dx.doi.org/10.1021/ja5097094 | J. Am. Chem. Soc. 2014, 136, 16128–16131

other molecular parameters, such as the identity of the metal ion, counterions, and ligand, can be varied to further improve the mechanical and self-healing properties of this new class of materials. These studies are currently undergoing in our laboratory, and the results will be reported in due course.

■ ASSOCIATED CONTENT

Supporting Information

All experimental details including sample preparation and characterization. This material is available free of charge via the Internet at http://pubs.acs.org.

■ AUTHOR INFORMATION

Corresponding Author

zguan@uci.edu

Notes

The authors declare no competing financial interest.

■ ACKNOWLEDGMENTS

This work was supported by the US Department of Energy, Division of Materials Sciences, under Award No (DE-FG02-04ER46162).

■ REFERENCES

(1) White, S. R.; Sottos, N. R.; Geubelle, P. H.; Moore, J. S.; Kessler, M. R.; Sriram, S. R.; Brown, E. N.; Viswanathan, S. *Nature* **2001**, *409*, 794.
(2) Ghosh, B.; Urban, M. W. *Science* **2009**, *323*, 1458.
(3) Chen, X.; Dam, M. A.; Ono, K.; Mal, A.; Shen, H.; Nutt, S. R.; Sheran, K.; Wudl, F. *Science* **2002**, *295*, 1698.
(4) Amamoto, Y.; Kamada, J.; Otsuka, H.; Takahara, A.; Matyjaszewski, K. *Angew. Chem., Int. Ed.* **2011**, *50*, 1660.
(5) Lu, Y.-X.; Guan, Z. *J. Am. Chem. Soc.* **2012**, *134*, 14226.
(6) Cordier, P.; Tournilhac, F.; Soulie-Ziakovic, C.; Leibler, L. *Nature* **2008**, *451*, 977.
(7) Burattini, S.; Greenland, B. W.; Merino, D. H.; Weng, W.; Seppala, J.; Colquhoun, H. M.; Hayes, W.; Mackay, M. E.; Hamley, I. W.; Rowan, S. J. *J. Am. Chem. Soc.* **2010**, *132*, 12051.
(8) Wang, Q.; Mynar, J. L.; Yoshida, M.; Lee, E.; Lee, M.; Okuro, K.; Kinbara, K.; Aida, T. *Nature* **2010**, *463*, 339.
(9) Phadke, A.; Zhang, C.; Arman, B.; Hsu, C.-C.; Mashelkar, R. A.; Lele, A. K.; Tauber, M. J.; Arya, G.; Varghese, S. *Proc. Natl. Acad. Sci. U.S.A.* **2012**, *109*, 4383.
(10) Wang, C.; Liu, N.; Allen, R.; Tok, J. B. H.; Wu, Y.; Zhang, F.; Chen, Y.; Bao, Z. *Adv. Mater.* **2013**, *25*, 5785.
(11) Yount, W. C.; Loveless, D. M.; Craig, S. L. *J. Am. Chem. Soc.* **2005**, *127*, 14488.
(12) Whittell, G. R.; Hager, M. D.; Schubert, U. S.; Manners, I. *Nat. Mater.* **2011**, *10*, 176.
(13) Holten-Andersen, N.; Harrington, M. J.; Birkedal, H.; Lee, B. P.; Messersmith, P. B.; Lee, K. Y. C.; Waite, J. H. *Proc. Natl. Acad. Sci. U.S.A.* **2011**, *108*, 2651.
(14) Yang, B.; Zhang, H.; Peng, H.; Xu, Y.; Wu, B.; Weng, W.; Li, L. *Polym. Chem.* **2014**, *5*, 1945.
(15) Burnworth, M.; Tang, L.; Kumpfer, J. R.; Duncan, A. J.; Beyer, F. L.; Fiore, G. L.; Rowan, S. J.; Weder, C. *Nature* **2011**, *472*, 334.
(16) Bode, S.; Zedler, L.; Schacher, F. H.; Dietzek, B.; Schmitt, M.; Popp, J.; Hager, M. D.; Schubert, U. S. *Adv. Mater.* **2013**, *25*, 1634.
(17) Hong, G.; Zhang, H.; Lin, Y.; Chen, Y.; Xu, Y.; Weng, W.; Xia, H. *Macromolecules* **2013**, *46*, 8649.
(18) Wang, Z.; Urban, M. W. *Polym. Chem.* **2013**, *4*, 4897.
(19) Fullenkamp, D. E.; He, L.; Barrett, D. G.; Burghardt, W. R.; Messersmith, P. B. *Macromolecules* **2013**, *46*, 1167.
(20) Maret, W.; Li, Y. *Chem. Rev.* **2009**, *109*, 4682.
(21) Chen, Y.; Kushner, A. M.; Williams, G. A.; Guan, Z. *Nat. Chem.* **2012**, *4*, 467.
(22) Moad, G.; Rizzardo, E.; Thang, S. H. *Aust. J. Chem.* **2009**, *62*, 1402.
(23) Skey, J.; O'Reilly, R. K. *Chem. Commun.* **2008**, 4183.
(24) Garcia-Bernabé, A.; Compañ, V.; Burguete, M. I.; García-Verdugo, E.; Karbass, N.; Luis, S. V.; Riande, E. *J. Phys. Chem. C* **2010**, *114*, 7030.
(25) Eisenberg, A.; Hird, B.; Moore, R. B. *Macromolecules* **1990**, *23*, 4098.
(26) A full investigation of M/L ratio on the materials performance will be reported elsewhere.